Computational Modeling of Battery Materials

Badri Narayanan

Department of Mechanical Engineering
University of Louisville
332 Eastern Parkway, Louisville, KY 40208 USA
Email: badri.narayanan@louisville.edu

ABSTRACT

This chapter provides a broad overview of the various computational modeling techniques used to gain fundamental insights into coupled electrochemical processes that occur in battery materials at electronic-to-mesoscopic scales. Representative successes of these techniques in modeling electrodes, electrolytes, and electrode-electrolyte interfaces are highlighted to establish the current state-of-the-art in the field.

KEYWORDS

Rechargeable batteries; Atomic-scale modeling; Density functional theory; Ab initio molecular dynamics; Reactive molecular dynamics; Classical molecular dynamics; Kinetic Monte Carlo; Solvation; Ion transport; Lithium intercalation; Solvate Electrolytes; Electrode-Electrolyte Interfaces; Modeling Electrochemical Reaction; Nucleation/growth of solid electrolyte interphases

INTRODUCTION

The ever-increasing demand for low-cost, safe, and high-density energy storage solutions for electric vehicles, consumer electronics, robotics, and electrical grids has necessitated development of new battery materials/chemistries at a rapid pace (Yu and Manthiram, 2017; Franco *et al.*, 2019). Such unprecedented rate of innovations cannot be sustained by traditional heuristic approaches involving expensive, time-intensive, and intuition-driven experiments alone (Jain *et al.*, 2013). With the high-performance computing facilities available today, computational modeling has emerged as an effective way to accelerate innovations in battery materials. This speed-up can happen in three ways: 1) computational screening of a vast library of battery-relevant materials to search for those with specific combination of desirable properties (e.g., electro-chemical stability, mechanical strength); 2) inverse design of materials by predicting a structure with prescribed properties; and 3) advancing the fundamental understanding of the physical factors underlying functionality of various battery components – all of which rely on an accurate description of complex electrochemical phenomena that occur in a typical battery.

The measurable electrochemical performance of battery, including its capacity, cycle life, rate capability, and Coulombic efficiency is governed by a complex hierarchy of electrochemical processes that occur over multiple length scales (**Figure 1**) (Franco *et al.*, 2019). For instance, the performance of a lithium ion battery relies on (a) stable (de)intercalation of Li^+ in the active material in the electrodes, which is governed by chemistry and lattice stability at sub-nanometer scale, (b) ion conduction through the bulk electrolyte, dictated by solvation dynamics over several nanometers, (c) nucleation/growth of passivating solid-electrolyte interphase (SEI), controlled by chemical reactions, electron transfer, and atomic transport over multiple scales, spanning Ångstroms to microns, and (d) charge/mass/heat transfer and stress distribution over continuum scales. Notably, all these processes are strongly and non-linearly coupled with each other. Consequently, a holistic understanding of the correlations between these processes, and their overall impact on functionality of a battery requires a multiscale modeling treatment. Owing to the immediate relevance of such computational strategies to the ever-growing battery community, numerous comprehensive reviews are already published focusing on individual modeling scales, including (a) first-principles approaches, (Urban, Seo and Ceder, 2016) (b) phase-field methods (Wang *et al.*, 2020), (c) linking the multiple modeling scales (Franco *et al.*, 2019), (d) understanding interfacial processes (Wang *et al.*, 2018) and (d) application of emerging machine learning tools, for various components of a battery (Guo *et al.*, 2021).

Among the various scales of materials, the electronic-to-mesoscopic regime that encompasses the spatiotemporal scales spanning 10^{-10}–10^{-6} meters and 10^{-15} – 10^{-4} seconds is particularly important for batteries, and constitutes the focus of this chapter. This regime features a rich variety of key electrochemical phenomena, including, solvation dynamics, ion transport, electron transfer, chemical reactions, structural transitions, and nucleation/growth of interphases – that are tightly coupled with each other, and strongly impact macroscale behavior of batteries, e.g., cycling performance, and degradation (Franco *et al.*, 2019). A wide range of materials modeling techniques are employed to access different regions in this spatiotemporal domain (**Figure 2**). In general, as the spatial/temporal resolution of the technique reduces, the complexity of the model reduces, and consequently, the associated computational time/costs become progressively smaller. Typically, each of the electrochemical processes is investigated using a different modeling technique that is best suited to access the necessary length/time scale (**Figure 2**).

Computational approaches based on quantum chemistry (QC) or first-principles provide most accurate predictions of material properties, often with errors on par with experiments; and are, thus, best suited for rapid computational screening of a library of materials. *Ab initio* molecular dynamics (AIMD), wherein interactions among electrons and nuclei are treated using Kohn-Sham density functional theory (DFT), can accurately describe molecular ordering around a metal ion (called solvation structures) in an organic liquid electrolyte, identify key chemical reactions, and assess their energetics as well as kinetic barriers. Classical atomic-scale approaches treat atoms as indivisible entities, and employs interatomic potential functions (or force fields, i.e., FFs) to describe the atomic interactions in terms of their positions relative to each other. Two kinds of FFs are commonly used, namely (a) reactive FFs that can capture the dynamics of formation/dissociation of chemical bonds, and associated charge transfer accurately, and (b) non-reactive

ones in which the connectivity between atoms remains fixed throughout the simulation. Reactive MD (RMD) simulations elucidate the mechanisms underlying intercalation/conversion dynamics, electrolyte decomposition, and formation of interphases at electrode-electrolyte interfaces. Non-reactive classical MD (CMD) reveal the critical links between solvation structure, ion aggregation and ionic conductivity. Mesoscopic coarse-grained MD (CGMD) approach further reduces the physical degrees of freedom of the system by defining a collection of atoms as an indivisible entity called beads; and describes dynamics in terms of interactions between these beads. Such techniques are critical to capture the slow relaxation dynamics of macromolecular segments in polymer electrolytes. Finally, material evolution over long time-scales ($>10^{-6}$ s) can be simulated using kinetic Monte Carlo (kMC) approach for a selected set of reactions/events sampled from AIMD/DFT/RMD simulations. Often, sequential linking multi-scale schemes are employed to unravel the relationship between processes occurring at different scales. In these schemes, processed output from a model at smaller scale (higher level of theory) is used to inform or train models at the next scale in the hierarchy. Usually, datasets derived from first principles (quantum theory) calculations are used to train classical force-fields, which are employed to perform CMD simulations at atomic-scale; dynamic properties obtained from CMD, in turn, are used as input to develop coarse-grained or MC models. In recent times, emerging techniques in machine learning (ML) have played a vital role in enabling rapid, robust, and seamless bridging of models across different length/timescales (Chan *et al.*, 2019b; Patra *et al.*, 2019; Chan *et al.*, 2019a; Narayanan *et al.*, 2017).

In this chapter, we introduce the reader to the various commonly employed approaches to model three main battery components, namely, (a) electrolyte, (b) electrode, and (c) electrode-electrolyte interface, within the electronic-to-mesoscopic regime. Representative examples from the literature are highlighted to establish the current state-of-the-art. Finally, we provide an outlook of the field with a few suggestions for future directions.

ELECTROLYTES

In any rechargeable battery, the electrolyte serves as a conduit to transport active ionic charge carriers between the electrodes, while the electrons flow through the external circuit. Owing to its central role in ion transport, design of electrolyte materials with a prescribed set of physical properties is crucial to engineer rechargeable batteries that offer high capacity-retention, long cycle life, good rate capability, and safety. Ideally, an electrolyte should exhibit (a) fast ionic conduction, (b) excellent electrochemical stability against high energy density electrodes (e.g., lithium nickel manganese cobalt oxide (NMC) cathodes and lithium anode), (c) low flammability, and (d) good thermomechanical robustness. Several concepts for high-performance electrolytes have been proposed to meet these needs, which can be broadly classified into three categories, namely, (a) organic liquids, (b) polymers, and (c) inorganic solids. Computational materials modeling techniques have accelerated design of electrolytes belonging to each of these categories by (a) enabling rapid screening of thousands of compounds for desirable physical properties using first-principles methods (with speed-up by ML) (Qu *et al.*, 2015; Narayanan *et al.*, 2019), and (b) providing a fundamental understanding of the dynamical processes associated with conduction of ionic charge carriers (e.g., Li^+ ion) through bulk electrolyte over multiple length/time scales (Franco *et al.*, 2019).

Organic Liquid Electrolytes

DFT (especially using B3LYP functional) has emerged as the standard method to compute thermochemical, solvation, and electronic properties of organic liquid electrolytes (Qu *et al.*, 2015; Narayanan *et al.*, 2019). High throughput infrastructures (such as Electrolyte Genome(Qu *et al.*, 2015)) utilize these first principles approaches within automated workflows to generate large databases of molecular properties relevant for battery electrolytes. For instance, using ~55,000 DFT-B3LYP calculations, Electrolyte Genome reported an open dataset of ionization potential (IP) and electron affinity (EA) for 4,830 possible organic electrolytes – two key properties, which (a) set the voltage limits within which a traditional Li ion battery can operate without any electrolytic decomposition, and (b) determine the operating voltage of a redox-flow battery(Qu *et al.*, 2015). Recently, similar infrastructures have been extended to compute energies for 133,296 organic molecules in GDB-9 database (that contain up to 9 C/N/O/F atoms, as well as H atoms) at chemical accuracy

(< 1 kcal/mol) using a high-level quantum chemistry composite method called G4MP2. The G4MP2 energies, in turn can accurately predict feasibility of millions of reaction pathways.(Narayanan *et al.*, 2019)

Large datasets from first-principles calculations provide (a) insights into links between the structure (motifs, chemical nature, and relative positioning of functional groups) and properties of molecules, as well as (b) a valuable resource to search for new organic liquids (present in the dataset) that possess desirable combination of molecular properties for use as an electrolyte. More importantly, these databases can be used to train fast-yet-accurate ML models to predict properties of large molecules that lie beyond the size-limitations of quantum-chemical methods. Indeed, G4MP2 dataset on 133,296 GDB-9 molecules enabled development of (a) fast ML models based on kernel-ridge-regression and deep convolution neural networks to provide accurate estimates of G4MP2 atomization energy of large molecules (> 10 non-hydrogen atoms) using their DFT-B3LYP energies (Ward *et al.*, 2019; Dandu *et al.*, 2020), and (b) graph neural networks to predict solvation energy of molecules in five solvents (acetone, ethanol, acetonitrile, dimethyl sulfoxide, and water) within 1 kcal/mol of those obtained from DFT-B3LYP calculations (Ward *et al.*, 2021). Such ML models, in turn, can be used to screen billions of organic molecules to identify promising electrolytes.

Typical liquid electrolytes used in batteries are solutions of a salt (e.g., $LiPF_6$) in an organic solvent (e.g., ethylene carbonate). Solvent molecules and salt anions present in liquid electrolytes tend to organize around ionic charge carriers (e.g., Li^+) forming solvation shells. Molecular structure of these shells as well as their atomic-scale dynamics govern ion transport through bulk electrolyte; and have, consequently, been the subject of numerous computational investigations. AIMD simulations indicate that Li^+ prefers a tetrahedral coordination in most organic electrolytes. However, the structure, composition, energetics, and dynamics of the solvation shell are controlled by the nature of salt/solvent as well as salt concentration. In particular, the relative energetics of (a) cation-anion interactions in the salt, and (b) cation-solvent interactions is of paramount importance to ion-transport (Tang, Tse and Liu, 2016; Franco *et al.*, 2019). Weak interactions between the salt cation and the solvent, such as that observed between Li^+ in $LiPF_6$ salt and diethyl carbonate (DEC) solvent allow the salt anion (PF_6^- in $LiPF_6$) to remain in the Li^+ solvation shell along with three solvent molecules. Consequently, Li^+ ion is forced to travel along with relatively slow-moving salt anion (PF_6^-) in the bulk electrolyte, resulting in low Li^+ ion conductivity. More importantly, such a *salt mediated* mechanism yields progressively lower Li^+ conductivity with increase in viscosity, severely restricting the range of amenable salt concentration. In contrast, solvents containing cyano- functional group (–CN), such as acetonitrile (AN), cause complete detachment of Li^+ from salt anion owing to strong interactions between Li^+ and N of –CN. This, in turn, allows Li^+ to move along with the solvent molecules without any impediment from the salt anions. Such a *solvent-mediated* diffusion mechanism facilitates fast Li^+ ion conduction even at high viscosity owing to Li^+ ion hopping between transient solvation shells (Tang, Tse and Liu, 2016). This finding opened the possibility of decoupling the effect of salt concentration and electrolyte viscosity on Li^+ conductivity; spurring design of super-concentrated electrolytes with high Li^+ ion conductivity and excellent thermal/electrochemical stability.

Super-concentrated (solvate) electrolytes feature unique network-like solvation structures composed of contact ion pairs, coordinated solvent molecules, and ion aggregates, like those elucidated by AIMD simulations of glyme (G*n*):LiTFSI electrolytes (**Figure 3(A-D)**). Such networks enable precise control over reaction pathways, solubility of intermediates, and electrolyte stability in emerging Li-S batteries. Specifically, they (a) exhaust the solvating power of the solvent to solvate any Li^+ ion belonging to Li-polysulfides, suppressing their dissolution and shuttle, (b) enable a quasi-solid-state speciation pathway that allows cell operation at low electrolyte-to-sulfur ratio (making Li-S batteries competitive with Li-ion on the basis of gravimetric energy), and (c) reduce solvent activity, which inhibits parasitic reactions at Li-anode (Pang *et al.*, 2018). Importantly, AIMD simulations indicate that the amount of free (uncoordinated) solvent can be carefully tuned with appropriate choice of solvent and concentration of salt in solvate electrolytes. For instance, among glyme:LiTFSI solvates, choosing a solvent diglyme (G2) similar in size to the salt anion ($TFSI^-$) results in a compact solvation shell, and minimizes the amount of free solvent (**Figure 3(E,F)**). The amount of free solvent is just enough to facilitate reaction kinetics, but not too high to promote deleterious reactions with Li-anode. In essence, the solvate electrolytes can address all key

barriers thwarting commercialization of Li-S batteries. Indeed, G2:LiTFSI (0.8:1) solvate electrolytes have enabled long-lived Li-S cells that retain high-capacity (~900 mAh/g) even after 100 cycles at low E/S ratios (~5 mL/g) (Pang *et al.*, 2018). Similarly, nominal amount of free solvent have been achieved with hydrofluoroether co-solvents to facilitate reaction kinetics in $(AN)_2$-LiTFSI solvates (Shin *et al.*, 2017). AIMD simulations have also been used to estimate solubility of Li_2O and LiO_2 in various organic solvents, which is crucial to gain insights into the charge-discharge processes of Li-O_2 batteries (Cheng *et al.*, 2017).

Long-time dynamics of solvation structure, solvent exchange, migration of ion clusters, salt aggregation; and their collective impact on conductivity of ionic charge carriers is best described by CMD simulations Careful analysis of CMD trajectories reveal two distinct modes of Li^+ migration: (a) vehicular diffusion, in which Li^+ ion moves along with its solvation shell, and (b) structural diffusion, in which Li^+ hops from one solvation shell to another via frequent exchange of mobile solvent molecules. Among these two modes, structural diffusion yields faster ion conduction (Borodin *et al.*, 2020). Competition between these two modes of diffusion depends on (a) cation-solvent binding energy, (b) solvent viscosity, and (c) salt aggregation. For instance, strong binding of Li^+ with ethereal oxygen atoms makes Li^+ transport in glyme-based electrolytes primarily vehicular. In contrast, the weaker interactions between Na^+ and ethereal oxygens enables frequent exchange of solvent molecules between neighboring solvation shell, rendering structural diffusion as the dominant transport mechanism for Na^+ ions in glymes (Borodin *et al.*, 2020). Weakly bound solvation shell around Al^{3+} in 1-ethyl-3-methylimidazolium chloride ([emim][Cl]) ionic liquid facilitate rapid ion association- dissociation, which allows rapid ion transport. CMD simulations with adaptive biasing force show that Al^{3+} solvation shell in [emim][Cl] (containing 6 Cl^- ions) has a free energy ~35 kcal/molecule lower than the solvation sheath in traditional 1:1 ethyl carbonate (EC): ethyl methyl carbonate (EMC) blend electrolyte (containing 3 EC and EMC molecules). The lower solvation free energy in [emim][Cl] results in largely structural diffusion, which enables ~3 times faster Al^{3+} conductivity in as compared to that in EC:EMC electrolyte, wherein Al^{3+} motion is vehicular (Kamath, Narayanan and Sankaranarayanan, 2014).

Polymer Electrolytes

Computational investigations on polymer electrolytes have been primarily focused on different variants of poly (ethylene oxide) (PEO) based electrolytes, including amorphous and crystalline forms, as well as those containing tethered anions and ceramic nanoparticles (Franco *et al.*, 2019). CMD simulations based on a polarizable FF show that PEOs form coordination loops around Li^+, which restrict the range of motion in polymer chains slowing down their dynamics. Notably, the slow motion of the polymer chains renders Li^+ motion sub-diffusive in amorphous PEOs over long times (30 – 40 ns) under ambient conditions, signaling the need for long timescales (100's of nanoseconds) to accurately describe Li^+ conduction in polymer electrolytes (Borodin and Smith, 2006). A typical approach to access such long timescales involves the use of CGMD simulations with interaction parameters derived from DFT or short all-atom CMD simulations.

CGMD simulations are extensively used to investigate the correlation between chain dynamics, ionic association, and structural order in polymer electrolyte. Importantly, these simulations have elucidated that percolation networks of polymer chains with ion aggregates preferably form in low dielectric constant ionomers (e.g., poly (ethylene-co-acrylic acid)). Such percolation networks enable fast Li^+ ion conduction through polymer electrolytes either via (a) continuous reformation of the network, or (b) collective motion of ion aggregates along the polymer chains (Hall, Stevens and Frischknecht, 2012; Franco *et al.*, 2019). Furthermore, CGMD simulations have also been employed to study the effect of solvent dilution and salt concentration on order-disorder transitions in block PEO-polystyrene (PS) copolymers. Neutral solvent diluents reduce the glass transition temperature by lowering the repulsive interactions between polymer blocks. On the other hand, at intermediate concentrations, salt ions stabilize PEO rich domains; and in turn, raise the transition temperature (Qin and de Pablo, 2016). These insights offer new principles to design block copolymers that feature both (a) stable blocks with high mechanical robustness, and (b) percolation networks of ion-aggregates facilitating fast Li^+ conduction.

Several models based on Monte-Carlo approaches have been used to obtain microscopic understanding of ion conduction in polymer electrolytes. Among these, the dynamic bond percolation (DBP) theory remains

the most popular owing to its simplicity. In the framework of DBP, Li^+ ion diffusion is treated as a random walk process, wherein Li^+ ions can hop between neighboring sites in a statistically disordered host lattice (polymer chains). The lattice itself undergoes dynamic re-arrangement owing to the orientational motion (or configurational entropy) of polymer chains. The model is characterized by two timescales, namely, (a) Li^+ hopping rate (fast), and (b) lattice renewal (slow) governed by local polymer relaxation dynamics (Druger, Nitzan and Ratner, 1983). Microscopic simulations based on DBP have been successfully employed to understand the effect of temperature and salt concentration on Li^+ conduction though polymer electrolytes. Another approach involves modeling the polymer chains as a one-dimensional lattice in which, Li^+ ions can move either by (a) hopping along a chain, (b) translate with chain segments, or (c) hop between chains; with probability of occurrence of each type of Li^+ move determined from short CMD runs. This microscopic transport model revealed that Li^+ hopping along PEO chains and Li^+ translation with PEO chain segments contribute equally to Li^+ conduction, while interchain hops are less important contributing merely ~10% to the overall Li^+ conduction (Borodin and Smith, 2006). Approaches combining DBP and microscopic transport models have also been proposed to understand the effect of polymer chain length on Li^+ conductivity (Franco *et al.*, 2019). Similarly, kinetic MC models based on key events identified by CMD simulations have been used to study the effect of nanoparticle fillers on Li^+ conduction in polymers (Franco *et al.*, 2019).

ML approaches have been recently employed to rapidly screen through a vast chemical space to identify promising polymer electrolytes. For instance, graph neural networks have been used to identify key structural features in polymers; these alongside gaussian process regression models have been used to learn the relationship between composition and experimentally measured conductivity for thousands of polymers. These newly developed ML models could successfully identify glassy polymers with high Li^+ conductivity (~10^{-3} S/cm) (Guo *et al.*, 2021)

Inorganic Solid Electrolytes

The growing safety concerns surrounding flammability of traditional organic liquid electrolytes has brought the inorganic solid-state superionic conductors, such as LISICON, NASICON, LiPON, garnet oxides, sulfides, and perovskites to the forefront (Nolan *et al.*, 2018). Until now, most computational efforts on understanding Li^+ ion conduction in bulk ceramic electrolytes have primarily focused on first-principles methods, including AIMD and DFT calculations. AIMD simulations are employed to sample different types of ion jumps, identify effect of temperature on ion-migration pathways, and understand effect of structure/composition on ion-migration. Nudged elastic band (NEB) calculations in the framework of DFT are employed to understand the physical factors underlying kinetic barriers for specific migration pathways (Nolan *et al.*, 2018). Using sulfide electrolytes as a representative class of solid electrolytes (SEs), AIMD simulations have elucidated that (a) defects promote Li^+ ion transport by reducing activation energy needed for hop and increasing charge carrier concentration in $Li_{10}GeP_2S_{12}$, (b) distribution of halogen (X) dopants among the available sites in Li_6PS_5X electrolytes has marked impact on Li^+ conductivity owing to subtle changes in the Li substructure around halogens or sulfur atoms, and (c) collective motion of Li^+ along with flexibility of P_2S_7 ditetrahedrals underlies superionic Li^+ conduction in $Li_7P_3S_{11}$ (Franco *et al.*, 2019). In perovskite oxides, Li^+ ion conduction follows a percolation pathway in A-site vacancies and is influenced by the structure and concentration of Li^+ ions. Interestingly, in a recent study integrating AIMD, DFT, and synchrotron experiments revealed that strongly correlated quantum effects can strongly influence Li^+ ion conduction. Specifically, in strongly correlated perovskite nickelates, Li^+ induces electron doping of a nearby Ni^{3+} in the perovskite lattice, which simultaneous causes (a) Mott transition into an electronically insulating phase, and (b) lattice expansion, which enables facile Li^+ diffusion. Such emergent physics provides a promising alternate pathway to design super-ionic conductors for other ions, such as Na^+ as well (Sun *et al.*, 2018).

MC and CMD simulations based on non-reactive classical pair potentials (with fixed atomic charges) have been used to extend the accessible length/time scales. For instance, MC and CMD simulations revealed the effect of grain boundary structure, and its impact on Li^+ ion migration in $Li_7La_3Zr_2O_{12}$ garnet electrolytes. These calculations showed that (a) the grain boundaries are enriched with Li, and (b) Li^+ diffusivity along

grain boundaries is lower than that in the bulk, but the extent of this decrease is sensitive to temperature and grain boundary structure (Yu and Siegel, 2017). The recent emergence of ML approaches in materials science has also enabled rapid computation of ion-diffusion behavior in solid state electrolytes. ML has primarily been used for three main purposes, namely (a) developing artificial neural network (ANN) potentials to describe atomic interactions from first principles datasets; these potentials are employed to run long-time MD simulations in complex solid electrolytes (including amorphous ones), (b) training ML models to directly predict conductivity based on structural features, without any MD simulations, and (c) developing ML models to identify new candidate materials based on key structural features in existing superionic conductors (Guo *et al.*, 2021).

ELECTRODES

Electrochemical performance of any battery, including its capacity, operating voltage, cyclability, and rate capability depends crucially on the physical properties of the active material used in the positive (cathode) and negative (anode) electrodes. Specific materials phenomena of interest include (a) thermodynamics of ion adsorption/desorption, (b) phase stability, (c) ion migration, (d) equilibrium voltage, and (e) microstructural evolution alongside associated stress distribution during battery cycling (i.e., lithiation/de-lithiation in lithium-ion batteries). A holistic understanding of these processes requires a combination of first-principles calculations, cluster expansion methods, AIMD/CMD simulations, statistical approaches (e.g., Monte Carlo), phase field and finite element calculations owing to the wide range of length/time scales associated with these processes. Below, we provide a brief discussion on the application of electronic-to-mesoscopic modeling techniques for electrode materials using Li-ion technology as a representative system. Detailed review of research progress on different aspects of modeling electrodes is available elsewhere.(Ma, 2018; Urban, Seo and Ceder, 2016)

Cathodes

In Li-ion batteries, typical positive electrodes serve as intercalation hosts for Li^+ ion, in which Li^+ ions are inserted during discharge, and extracted when the battery is charged. Several classes of transition metal oxides, including layered (e.g., $LiCoO_2$), spinel (e.g., $LiMn_2O_4$), tunneled oxides (e.g., MnO_2), and polyanionic frameworks (e.g., $LiFePO_4$) have been proposed and investigated as cathode materials (Franco *et al.*, 2019; Urban, Seo and Ceder, 2016; Ma, 2018). Ideally, the structure of these hosts should remain largely intact during intercalation/de-intercalation of Li^+ ions; however, phase changes via lattice distortions (beyond certain Li amount) have been observed in most electrodes. Hubbard-corrected DFT+*U* calculations are used to evaluate formation energies for various possible host structures at any given concentration of Li; the phases (or linear combination of phases) with the lowest energy at different composition are connected to construct the convex hull (Urban, Seo and Ceder, 2016). This convex hull shows the most energetically stable structure at any Li-content and provides insight into energetics of structural/phase evolution during charge/discharge of Li-ion battery (lithiation/de-lithiation). Convex hull construction based on DFT+*U* was recently used to investigate the effect of stabilizing K^+ cations on structural transitions in tunneled MnO_2 cathodes during lithiation (**Figure 4**) (Kempaiah *et al.*, 2021). These calculations showed that at low K^+ concentrations (e.g., KMn_8O_{16}), Li^+ ions preferentially intercalate into *8h* sites in empty tunnels (that do not contain K^+) to avoid electrostatic repulsive interactions with K^+. In fact, convex hull analysis indicated that these electrolytes undergo lithiation by first intercalating 4 Li^+ ions in the empty tunnels, before inserting Li^+ ions in the K^+ tunnels (**Figure 4A,B)**. Such a lithiation pathway allows the tunneled structure to remain stable up to high Li^+ insertions (Li/Mn ~0.75), at which point tunneled structure begins to transform to layered one (**Figure 4B)**. The ability of KMn_8O_{16} to host more Li^+ per transition metal without structural change would enable higher capacity, and better cyclability. However, at high K^+ concentrations, $K_2Mn_8O_{16}$, empty tunnels are not available for Li^+ to intercalate. Consequent electrostatic repulsions between K^+ and Li^+ ions in the tunnels causes significant structural distortion, causing transition to layered form at lower levels of Li insertion (Li/Mn ~0.375) and subsequent amorphization (Li/Mn ~0.625); these structural transitions hamper cyclability of these cathodes (**Figure 4C)**. Formation energies of the stable phases from the convex hull at different Li concentration can be used to predict the cell voltage

profile (with respect to Li/Li^+) in good agreement with experiments (**Figure 4D**). For $K_yMn_8O_{16}$ cathode, lithiation can be represented as: $K_yMn_8O_{16} + xLi \rightarrow Li_xK_yMn_8O_{16}$. The cell voltage can be evaluated as:

$$V = -\left(E_{\{Li_xK_yMn_8O_{16}\}} - E_{\{K_yMn_8O_{16}\}} - x.E_{\{Li\}}\right)/(x.e),$$

where $E_{\{Li_xK_yMn_8O_{16}\}}$, $E_{\{K_yMn_8O_{16}\}}$, $E_{\{Li\}}$ are the ground-state formation energies of the lithiated $Li_xK_yMn_8O_{16}$, unlithiated $K_yMn_8O_{16}$, and body-centered cubic Li, while *e* is the charge on an electron. NEB calculations in the framework of DFT+*U* give insights into the kinetic barriers associated Li^+ transport within the electrode. A more facile Li^+ migration is indicative of good rate capability of the electrode. For instance, increased K^+ doping results in higher Li-migration barriers, which in turn, signifies lower rate capability (**Figure 4E**). Electronic structure calculations show that K^+ doping introduces semi-metallicity, which could enhance the capacity and rate capability of $K_yMn_8O_{16}$ tunneled cathodes (Kempaiah *et al.*, 2021).

To understand the effect of temperature on the phase diagram of Li-TM-O (TM: transition metal), cluster expansion models are developed using formation energies obtained from DFT+*U*. These models are then used to empower grand-canonical MC or kMC simulations to investigate the effects of finite temperature on phase stability, and Li/vacancy ordering (Urban, Seo and Ceder, 2016; Ma, 2018; Franco *et al.*, 2019). Similarly, kMC simulations informed by DFT+*U* energetics have been used to explore the kinetics of phase evolution in $LiFePO_4$ cathodes during lithiation/de-lithiation. Integrating DFT+*U*, cluster expansion. And kMC simulations has enabled identifying the effect of temperature, vacancy distribution, and Li concentration on the Li^+ diffusion in layered $LiTiS_2$. These studies indicated that Li^+ migration is (a) dominated by hops between neighboring octahedral sites in TiS_2, and (b) promoted by presence of divacancies (Van der Ven *et al.*, 2008). Additionally, AIMD simulations have also been used to investigate Li^+ diffusion pathways in several cathode materials. The structural, thermodynamic, and kinetic properties deduced from these electronic-to-mesoscopic simulations have been used to evaluate the parameters in continuum scale formulations, such as phase-field coupled with mechanics and Butler-Volmer electrochemical kinetics (Srinivasan *et al.*, 2018). Such frameworks provide a pathway to investigate the relationships between microstructure evolution, stress distribution, and cell voltage. Detailed discussion of such continuum approaches is out of scope of this chapter and are available elsewhere (Srinivasan *et al.*, 2018).

Recently, ML approaches have been employed to (a) train ANN potentials for complex cathodes (e.g., $LiNi_xMn_yCo_{(1-x-y)}O_2$) using training set derived from DFT to predict phase stability, thermodynamics of defect ordering, and cell voltage, (b) estimate Li^+ migration barriers by learning-on-the-fly, (c) develop quantitative structure-property relationships, and (d) develop predictive models that can screen vast number of compounds for desired cell voltage based on simple features (Guo *et al.*, 2021).

Anodes

Graphitic carbon-based materials remain most popular choice for use as anodes in LiBs owing to their low voltage with respect to Li, low cost, abundance, and long cycle life. Like for the cathodes, a combination of DFT, cluster expansion, and MC methods have been used to investigate the thermodynamics of Li ordering within graphite. Importantly, these studies revealed that Li insertion in graphite is governed by the competition between (a) electrostatic repulsion among intercalating Li^+ ions, and (b) van der Waals attraction between atomic layers of graphite. The tug-of-war between these two opposing factors precludes homogeneous insertion of Li^+ ions within graphite during lithiation (Persson *et al.*, 2010). Depending on the concentration of Li, either one or two empty layers of graphite can exist between Li-filled layers. A combination of DFT-NEB and kMC simulations elucidated the effect of Li concentration on Li^+ diffusion along the graphitic planes. These studies indicated that although Li^+ conduction within graphitic planes is quite fast (10^{-7} to 10^{-6} cm^2/s), grain boundaries can drastically impede Li^+ diffusion (~10^{-11} cm^2/s) (Persson *et al.*, 2010). First-principles simulations have also been employed to understand lithiation behavior in beyond-graphene anode materials, such as amorphous $SiO_{1/3}$. AIMD simulations have shown that high Li/Si ratio (~4) can be achieved in oxygen-deficient silica anodes by carefully tuning the O distribution and Si/O ratio (Chou and Hwang, 2013). Reactive MD simulations provide an effective route to access the

length/time-scales necessary to explore the energetics, dynamics, and mechanics associated with lithiation/de-lithiation process in low-dimensional (e.g., onion like carbon) or amorphous materials. Grand canonical MC and MD simulations based on a reactive force field (ReaxFF) showed that vacancies provide energetically preferred sites for Li adsorption in graphitic carbon. As the number of vacancies in graphitic carbon increase, the Li/C ratio increases yielding higher cell voltages at all lithiation levels. Additionally, these atomic-scale simulations also revealed that zero-dimensional onion-like carbon facilitate fast charging/discharging rates by providing numerous sites for Li adsorption/desorption in the outer layers, demonstrating the promise of onion-like carbon for anode applications (Raju *et al.*, 2015). Similarly, reactive MD simulations have elucidated the atomic-scale mechanisms underlying mechanical response of amorphous Li_xSi alloys under a variety of chemo-mechanical loading conditions, with implications for Si anodes (Fan *et al.*, 2013).

ML models based on gaussian process regression developed using *ab initio* datasets have been used to study amorphization and battery performance in graphitic anodes. Similarly, ANN potentials (alongside evolutionary sampling) have been used to (a) identify low-energy atomic configurations over the entire range of compositions in amorphous Li_xSi, which yield average voltage values consistent with experiments, and (b) elucidate mechanisms underlying Li diffusion and Si segregation during de-lithiation of amorphous Li-Si nanoparticles. Insights from these simulations offer guidelines to design Si-based anodes with enhanced rate-capability (Guo *et al.*, 2021).

ELECTRODE-ELECTROLYTE INTERFACES

The primary redox reactions underlying the operation (i.e., charge/discharge) of a battery rely on steady transfer of ions to and from the electrode across the boundary region (few tens of nanometer thick) between electrode and electrolyte, called electrode-electrolyte interfaces. Consequently, the electrochemical performance of a battery (i.e., capacity, rate capability, and cycle life) is intimately tied to the thermodynamics, reactivity, electron/ion conduction, and mechanics at these interfaces. Evidently, a fundamental understanding of structure-property-performance relationships at electrode-electrolyte interfaces is crucial to accelerate design of high-performance battery technologies. Computational modeling at electronic-to-mesoscopic scales has been instrumental in elucidating such relations by providing insights into several interconnected interfacial phenomena, including, chemical reactions, solvation dynamics, atomic diffusion, charge transport, and microstructural evolution.

Anode-Electrolyte Interfaces

Nominal decomposition of the electrolyte is inevitable at electrified interfaces in any rechargeable battery, owing to the metastable nature of electrolytes under typical voltages of battery operation. Especially, at the anode-electrolyte interface, products arising from electrolyte decomposition form a passivating layer, called the solid electrolyte interphase (SEI), which is widely regarded as the key enabler of rechargeable battery technologies (Franco *et al.*, 2019). A perfect SEI should prevent continuous electrolyte decomposition by hindering electron flow, while still allowing rapid conduction of primary charge carrying ions (e.g., Li^+ in Li-ion battery). Realization of such a SEI requires a clear understanding of the elementary steps underlying the initial formation of SEI and subsequent growth during cycling, as well as identifying key structure-property relationships. Specifically, it is necessary to delineate the effect of (a) solvents, co-solvents, salts, and additives in the electrolyte, and their relative amounts, (b) chemistry, structure, and morphology of the anode, and (c) operating conditions (e.g., voltage, C-rate, temperature) on the structure, composition, and physical properties of the SEI.

AIMD simulations have been successfully used to identify the mechanisms underlying initial stages of degradation of liquid electrolytes (up to ~100 ps) upon contact with commonly used anodes, including lithium metal, graphite, silicon, and tin (Franco *et al.*, 2019). Most studies have focused on interfaces with carbonate electrolytes (primarily EC) due to their prevalence in conventional Li-ion batteries. AIMD simulations reveal that EC decomposes on Li (001) to form SEI via a sequential transfer of two electrons from anode to EC. This two-electron mechanism can either cause stepwise dissociation of two bonds between (a) the carbonyl C and two O atoms of the ring, resulting in a $O(C_2H_4)O_2^-$/CO pair, which

subsequently reacts with two CO_2 molecules to form ethylene decarbonate; or (b) ethylene C and ring O to form C_2H_4/CO_3^{2-}pair. Both pathways have similar reaction barriers, indicating that they are equally likely (Leung *et al.*, 2011; Brennan *et al.*, 2017). However, AIMD simulations show that EC rearranges into a bent geometry near Li or graphite anode, which is more amenable to decomposition via the first pathway yielding $O(C_2H_4)O_2^-$/CO pair (Leung *et al.*, 2011). Similar decomposition of EC has also been reported for graphite, silicon, and tin anodes (Franco *et al.*, 2019). Interestingly, AIMD simulations show that the nature of edge terminations in graphite control the decomposition products, e.g., (a) edge C=O facilitate EC decomposition to form $O(C_2H_4)O_2^-$/CO or C_2H_4/CO_3^{2-} pairs, (b) edge C-OH forms ethylene glycol via EC degradation followed by H^+ transfer, while (c) edge C-H terminations do not cause breakdown of EC. Breakdown of anions (e.g. $TFSI^-$) in electrolyte salt also contributes to SEI formation(Leung and Budzien, 2010). AIMD simulations indicate that $TFSI^-$ salt anions provide sacrificial protection to a range of solvents (e.g., glymes, AN, ionic liquids) from reductive decomposition against Li anode by forming an amorphous SEI containing LiF, Li_2O, as well as S, N, and C anions bonded with Li (Merinov *et al.*, 2019).

Understanding dynamical processes underlying formation, composition, and atomic-structure of SEI requires access to larger length/time scales (10's of nm and few ns) that are afforded by RMD simulations in the framework of ReaxFF trained using first-principles datasets. RMD simulations have elucidated the distribution of various species in the SEI formed in traditional Li^+ ion batteries with carbonate electrolytes (EC, and dimethyl carbonate (DMC)). These simulations showed that SEI consists of two layers: (a) an outer layer containing organic salts, and (b) an inner layer made up of inorganic salts, consistent with experimental reports. Importantly, they indicate that lithium butylene dicarbonate (LiBDC) can form in the initial stages by combination of two EC^- radicals releasing a C_2H_4; subsequently, LiBDC decomposes into Li_2CO_3 and Li_2O in Li-rich regions. DMC is less reactive against Li than EC, as evidenced by presence of partially reduced products, such as $LiOCH_3$ and $LiOCO_2CH_3$, in the SEI (Kim, Duin and Shenoy, 2011). RMD simulations have also been employed to assess the effectiveness of additives in preventing solvent decomposition. Recently, the formalism of ReaxFF has been extended to explicitly describe electron transfer events using a pseudo-classical treatment.(Islam *et al.*, 2016) This extended framework, called eReaxFF, shows that electron transferred from Li anode to EC localizes between the C and O atoms in the ring causing these bonds to break. Subsequent reactions of the EC^- radical depend on its concentration; presence of several EC^- radicals in close proximity results yields Li_2BDC or Li_2EDC alongside release of C_2H_4 (Islam *et al.*, 2016). Non-reactive CMD simulations are used to investigate ion conduction in as-formed SEI layers. For instance, CMD simulations using polarizable FFs show that (a) Li^+ diffusion in ordered SEI made up of Li_2EDC is 2-3 times higher than that in amorphous SEI, and (b) presence of long alkyl chain spacers between carbonate groups (e.g., in Li_2BDC vs Li_2EDC) promotes ordered SEI, albeit with reduced stiffness, which cannot suppress dendrite growth (Bedrov, Borodin and Hooper, 2017). Furthermore, using key reaction paths identified by AIMD/RMD simulations, hybrid MD/MC and kMC approaches have been used to investigate growth of SEI during battery cycling over mesoscopic length/timescales (Franco *et al.*, 2019).

The success of emerging solid-state battery technology is also irrevocably tied to the reactivity, and ion/electron transport across anode-SE interfaces. Most efforts on solid-state anode-electrolyte interfaces have focused on either (a) phase stability of SEs at different lithiation levels using convex hulls constructed in the framework of DFT following similar techniques as discussed earlier for electrodes (Schwietert, Vasileiadis and Wagemaker, 2021), or (b) AIMD simulations to identify the initial reactions at the interface (Galvez-Aranda and Seminario, 2019). The thermodynamics and kinetics of ion/electron transfer across a solid anode-electrolyte interface is controlled by a space charge layer made up of point defects, also known as the electrical double layer (EDL). To capture spatial variation of (a) defect concentration and (b) electrochemical potential across the EDL, a general mathematical model based on Poisson-Fermi-Dirac equation has been proposed, which treats electronic band bending and point defect formation energies (obtained from DFT) in a self-consistent manner (Swift, Swift and Qi, 2021). This model enables determination of optimal thickness for any given interlayer material (e.g., LiF, Li_2CO_3) to minimize the electrostatic barrier for Li-ion transport across anode-SE interface (e.g., interface between Li and

$Li_7La_3Zr_2O_{12}$). The key driving forces identified by such models can also be integrated with CMD simulations to unravel atomistic details of the EDL (Swift, Swift and Qi, 2021). Recently, ML approaches have been employed to (a) identify the structure of energetically stable SEI with complex electrolytes (e.g., $Li_{1.3}Al_{0.3}Ti_{1.7}(PO_4)_3$), (b) investigate relationship between their structure, ionic-conductivity and mechanical properties, and (c) predict promising coating materials with superionic conduction (Guo *et al.*, 2021).

Cathode-Electrolyte Interfaces

On the cathode side, an analogous cathode-electrolyte interphase (CEI) forms, whose characteristics vary significantly depending on the chemistry of the active material in the cathode. Apart from electrolyte decomposition, cathodes introduce a rich variety of unique processes, including structural transitions in cathode, transition metal leaching, and gas evolution that govern structural evolution of CEI (as well as its physical properties). Owing to the vast array of distinct cathode chemistries used in batteries today, and their inherent complexity, computational studies on CEI are relatively scarce (Yu and Manthiram, 2017). Most works have focused on using AIMD simulations to understand (a) decomposition of EC, and (b) the role of Mn disproportionation in Mn dissolution at interfaces between $Li_xMn_2O_4$ spinel cathodes and carbonate electrolytes (Leung, 2012). Additionally, AIMD simulations have also been employed to study reactions between sulfur cathodes and various solid state sulfide electrolytes (Camacho-Forero and Balbuena, 2018). ML approaches have also been recently employed to study the structure, ionic conductivity, and mechanical properties of CEI (similar to SEI), particularly for Li-P-S electrolytes with typical cathode $LiCoO_2$ (Guo *et al.*, 2021).

OUTLOOK

Computational modeling at electronic-to-mesoscopic scales have elucidated the molecular-scale dynamics underlying a wide range of key electrochemical phenomena relevant to batteries, especially for idealized electrodes, bulk electrolytes, and electrode/electrolyte interfaces. Equally important, high throughput searches based on first-principles have even led to discovery of promising new electrolyte chemistries, high-voltage cathode materials, and superionic conducting solid-state electrolytes. Nevertheless, challenges still persist with respect to modeling electrode-electrolyte interfaces, especially (a) interfaces between Li-metal anode, and emerging organic electrolyte chemistries, (e.g., room temperature ionic liquids and solvate electrolytes) and complex solid-state electrolytes (e.g., sulfide electrolytes), and (b) cathode-electrolyte interfaces. In addition, understanding molecular processes underlying thermodynamics/kinetics of ion de-solvation at electrified electrode-electrolyte interfaces holds the key for designing materials for fast charging rechargeable batteries; yet, such knowledge is still in its infancy. Most efforts till now have focused on first-principles based approaches. AIMD simulations have identified key reactions governing initiation of SEI/CEI for ideal electrode-electrolyte interfaces (Merinov *et al.*, 2019; Camacho-Forero and Balbuena, 2020; Leung, 2012). Similarly, AIMD simulations coupled with rare-event sampling methods (e.g., blue moon ensemble) have unraveled (a) transition states, (b) free energy profiles, and (c) activation energy associated with de-solvation of Li ions at the interface between Si anode and propylene carbonate electrolyte under applied bias (Ohwaki *et al.*, 2018).

Notwithstanding the key insights provided by first principles approaches, they cannot access the length/timescales necessary to understand the effect of salt, additives, and solvents in emerging organic electrolytes or stoichiometry of SEs on (a) formation processes, (b) structure, morphology, and composition, as well as (c) structure-property relationships of SEI/CEI. Similarly, *ab initio* techniques cannot probe the effect of (a) electrolyte composition, and (b) structure, morphology, and composition of SEI/CEI, on ion de-solvation. CMD simulations based on reactive FFs alongside advanced rare-event sampling methods provide an effective route to access the necessary length/time scales; however, such FFs are not available. ML methods based on gaussian process regression, kernel ridge regression, and artificial neural networks, as well as automated FF-development workflows can enable rapid training of these classical FFs from first-principles datasets (Patra *et al.*, 2019; Chan *et al.*, 2019b). Such ML-assisted bridging of spatiotemporal scales in modeling would also be helpful to investigate lithium-excess cathode

materials that exhibit partial cation disorder, and non-coherent structural transitions with stoichiometric changes (Urban, Seo and Ceder, 2016).

As ML based techniques become more popular with the battery modeling community, two key issues need to be addressed: 1) incorporation of physics into ML models to enhance their transferability, 2) collecting, curating, and maintaining an open database of materials properties calculated from first principles and/or experiments (similar to Materials Project (Jain *et al.*, 2013)).

Lastly, another key area that deserves attention is the link between models at electronic-to-mesoscale with continuum scale approaches, including phase-field, Butler-Volmer frameworks. Recent works have already reported using DFT/AIMD/CMD simulations to extract key materials parameters (e.g., interfacial energies, fracture strength, grain boundary energy etc.) needed for these continuum simulations to investigate dendrite growth in LLZO electrolyte, and delamination of transition-metal oxide cathodes ($LiNi_{0.8}Mn_{0.1}Co_{0.1}O_2$ and $LiCoO_2$) against LLZO, as well as its effect on the capacity fade in battery (Barai *et al.*, 2021; Barai *et al.*, 2020). Such efforts become even more meaningful when considered in the context of increasing availability of automated or robotic high-throughput synthesis/characterization (Dave *et al.*, 2020). Continuum scale models informed by atomic-scale simulations can help speed-up Bayesian-optimization methods to guide the robotic synthesis and drastically reduce the number of experiments.

ACKNOWLEDGEMENT

This work was supported by the U. S. Department of Energy (DOE), Office of Energy Efficiency and Renewable Energy (EERE), Vehicle Technologies Office under Award #EE0008866. The author also acknowledges support from Oak Ridge Associated Universities (ORAU) through the Ralph E. Powe Junior Faculty Enhancement Award.

FIGURES AND TABLES

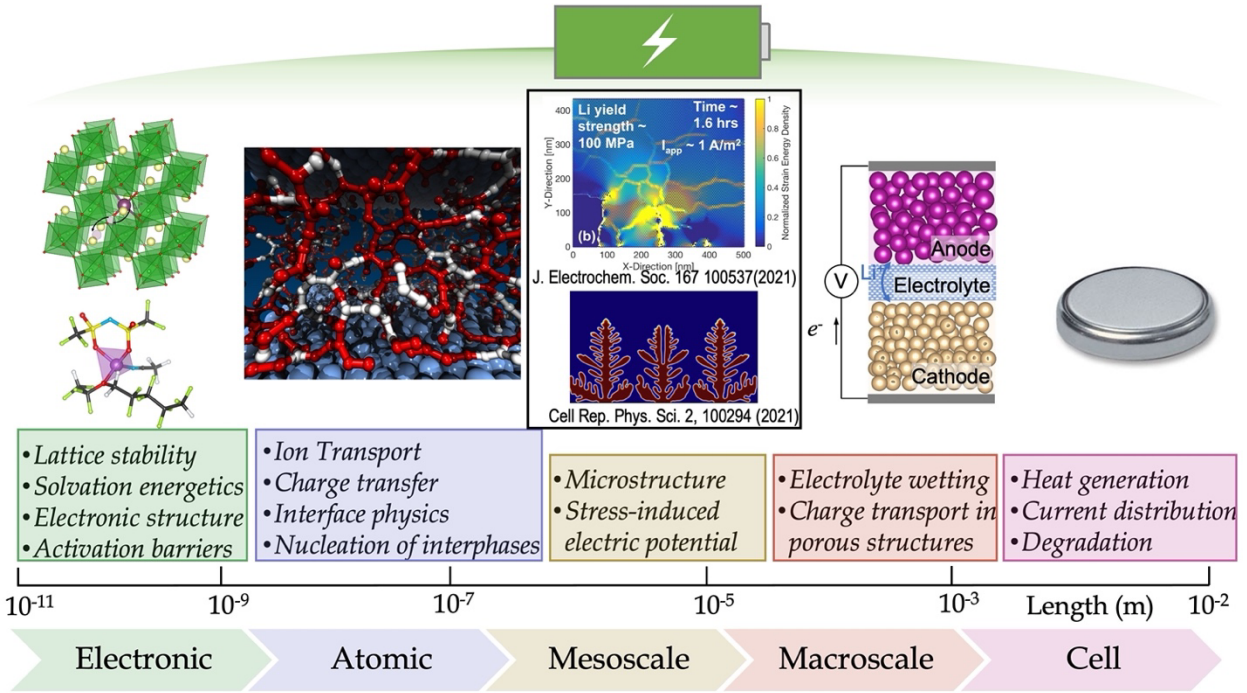

Figure 1. Schematic representation of the hierarchy of coupled electrochemical phenomena that occur in rechargeable batteries over multiple scales. The pictures enclosed in the black rectangle are (Top) Adapted with permission from Journal of Electrochemical Society, Barai *et al.*, "The role of local inhomogeneities on dendrite growth in LLZO-based solid electrolytes",167, 100537 (2021) © The Electrochemical Society. Reproduced by permission of IOP Publishing Ltd. All rights reserved (Bottom) Reprinted from Cell Reports Physical Science, Z. Liu *et al.*, "Dendrite-free Lithium Based on Lessons Learned from Lithium and Magnesium Electrodeposition Morphology Simulations", 2, 100294 Copyright (2021), with permission from Elsevier.

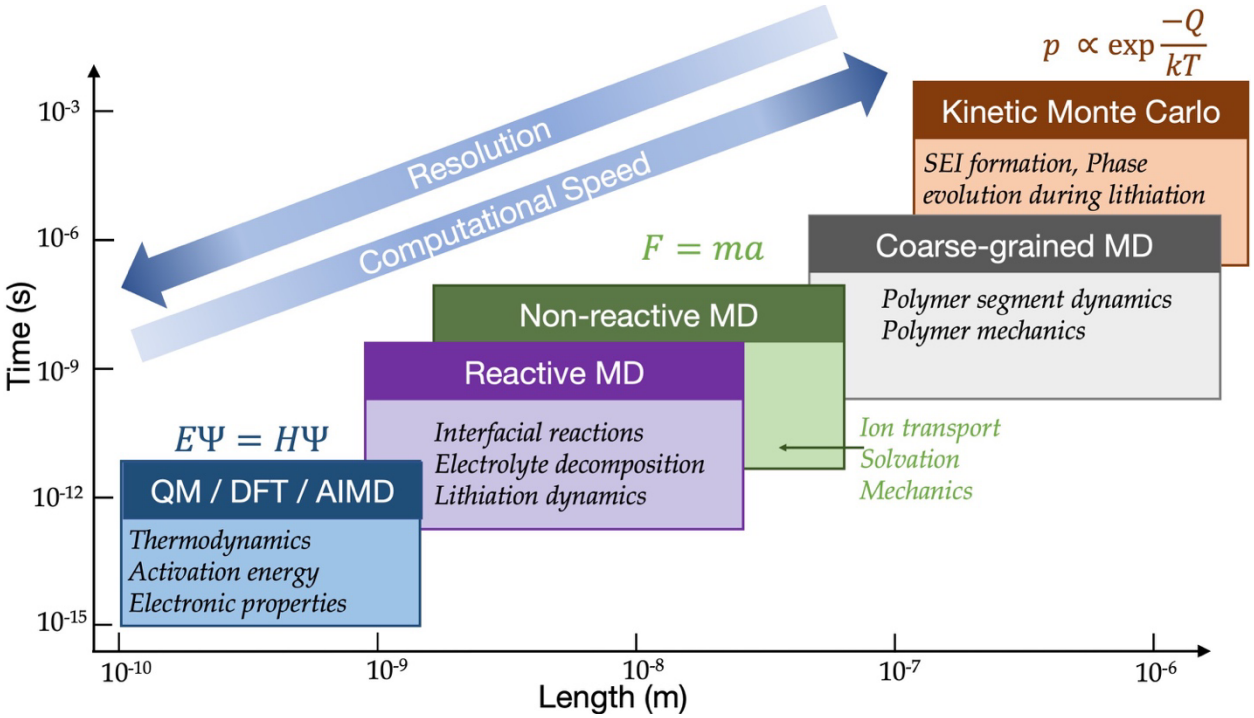

Figure 2. Length and time scales for various computational materials modeling techniques within the electronic-to-mesoscopic regime.

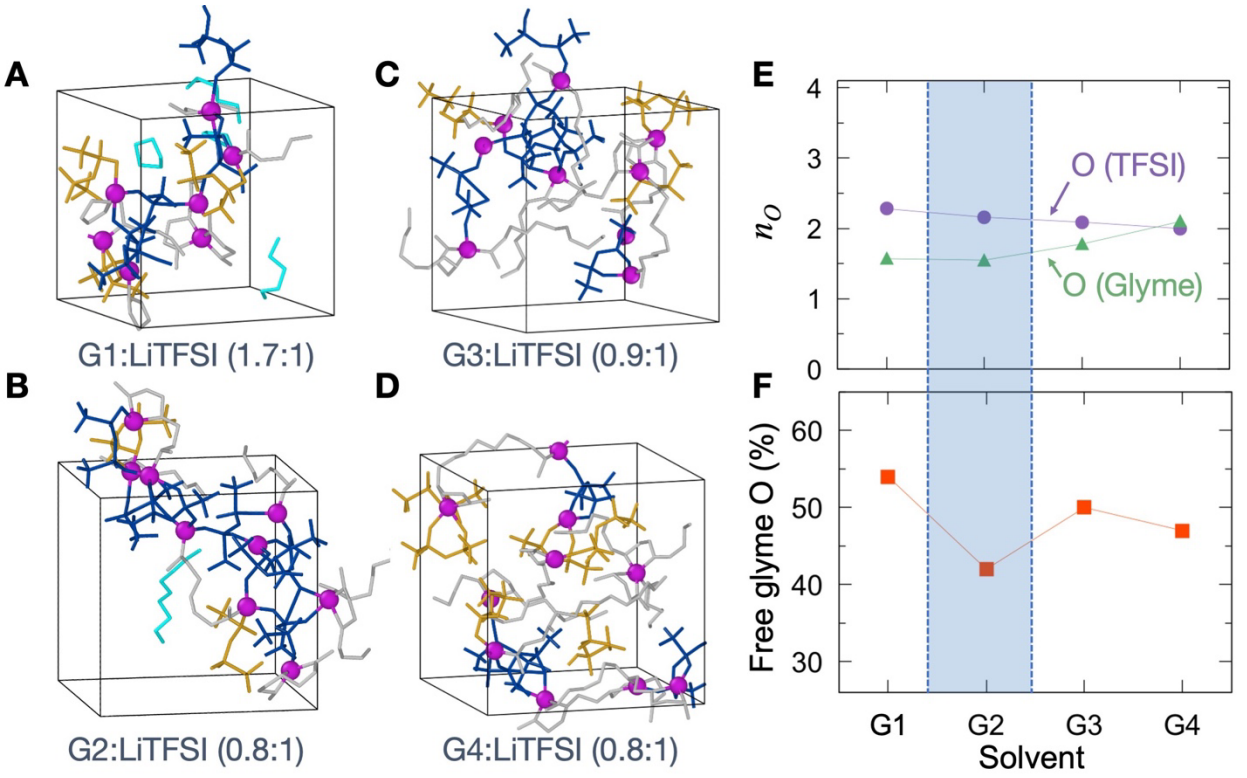

Figure 3. AIMD simulations show that glyme based solvate electrolytes form solvation networks around Li^+. Typical AIMD snapshots are shown for (A) (1.7:1) G1: LiTFSI, (B) (0.9:1) G3:LiTFSI, (C) (0.8:1) G2:LiTFSI, and (D) (0.8:1) G4:LiTFSI. Oxygen coordination around Li^+ ions in the first solvation shell is analyzed to identify (E) number of O neighbors arising from TFSI- and glyme, and (F) fraction of O atoms in the glyme that are free, i.e., are not coordinated by any Li^+ cation. In panels (A-D), Li^+ cations are shown in purple, free and coordinated glyme molecules are marked in gray and cyan respectively, while contact-ion pairs (CIP), and aggregates of TFSI- anions are shown in gold and blue respectively; hydrogen atoms are not displayed for the sake of clarity. In panels (E-F), the optimal size of the glyme that leads to minimum free solvent is highlighted by the blue rectangle. [Reproduced with permission from Nature Energy, "Tuning the electrolyte network structure to invoke quasi-solid state sulfur conversion and suppress lithium dendrite formation in Li–S batteries", Pang *et al.*, 3, 783–791 (2018), Copyright © 2018, Q. Pang, A. Shyamsunder, B. Narayanan, C.Y. Kwok, L. A. Curtiss and L. F. Nazar]

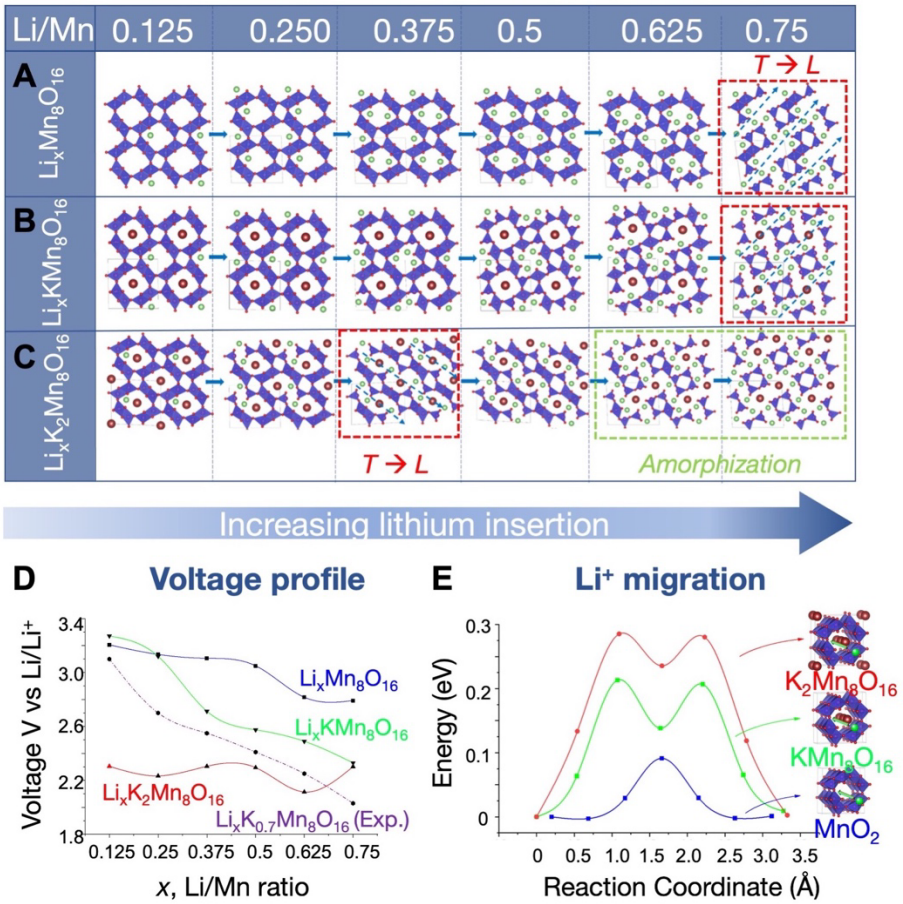

Figure 4. First principles investigation of lithiation behavior of $K_yMn_8O_{16}$ cathodes (y = 0-2). Ground state structures at different stages of lithiation (as described by Li/Mn content) for (A) $Li_xMn_8O_{16}$, (B) $Li_xKMn_8O_{16}$, and (c) $Li_xK_2Mn_8O_{16}$ obtained using convex hull construction from DFT calculations. (D) Voltage discharge profile predicted by DFT calculations for $Li_xMn_8O_{16}$ (blue), $Li_xKMn_8O_{16}$ (green), and $Li_xK_2Mn_8O_{16}$ (red) as compared to experiments for $Li_xK_{0.7}Mn_8O_{16}$ (purple). (E) Activation barrier for Li+ ion transport in Mn_8O_{16} (blue), KMn_8O_{16} (green), and $K_2Mn_8O_{16}$ (red) obtained using DFT-NEB calculations. [Adapted with permission from Kempiah et al., "Impact of Stabilizing Cations on Lithium Intercalation in Tunneled Manganese Oxide Cathodes", ACS Applied Energy Materials, Article ASAP, DOI: 10.1021/acsaem.1c01598}. Copyright 2021 American Chemical Society.]

REFERENCES

Barai, P., Ngo, A. T., Narayanan, B., Higa, K., Curtiss, L. A. and Srinivasan, V. (2020) 'The Role of Local Inhomogeneities on Dendrite Growth in LLZO-Based Solid Electrolytes', *Journal of The Electrochemical Society,* 167(10), pp. 100537.

Barai, P., Rojas, T., Narayanan, B., Ngo, A. T., Curtiss, L. A. and Srinivasan, V. (2021) 'Investigation of Delamination-Induced Performance Decay at the Cathode/LLZO Interface', *Chemistry of Materials*.

Bedrov, D., Borodin, O. and Hooper, J. B. (2017) 'Li+ Transport and Mechanical Properties of Model Solid Electrolyte Interphases (SEI): Insight from Atomistic Molecular Dynamics Simulations', *The Journal of Physical Chemistry C,* 121(30), pp. 16098-16109.

Borodin, O., Self, J., Persson, K. A., Wang, C. and Xu, K. (2020) 'Uncharted Waters: Super-Concentrated Electrolytes', *Joule,* 4(1), pp. 69-100.

Borodin, O. and Smith, G. D. (2006) 'Mechanism of Ion Transport in Amorphous Poly(ethylene oxide)/LiTFSI from Molecular Dynamics Simulations', *Macromolecules,* 39(4), pp. 1620-1629.

Brennan, M. D., Breedon, M., Best, A. S., Morishita, T. and Spencer, M. J. S. (2017) 'Surface Reactions of Ethylene Carbonate and Propylene Carbonate on the Li(001) Surface', *Electrochimica Acta,* 243, pp. 320-330.

Camacho-Forero, L. E. and Balbuena, P. B. (2018) 'Exploring interfacial stability of solid-state electrolytes at the lithium-metal anode surface', *Journal of Power Sources,* 396, pp. 782-790.

Camacho-Forero, L. E. and Balbuena, P. B. (2020) 'Elucidating Interfacial Phenomena between Solid-State Electrolytes and the Sulfur-Cathode of Lithium–Sulfur Batteries', *Chemistry of Materials,* 32(1), pp. 360-373.

Chan, H., Cherukara, M. J., Narayanan, B., Loeffler, T. D., Benmore, C., Gray, S. K. and Sankaranarayanan, S. K. R. S. (2019a) 'Machine learning coarse grained models for water', *Nature Communications,* 10(1), pp. 379.

Chan, H., Narayanan, B., Cherukara, M. J., Sen, F. G., Sasikumar, K., Gray, S. K., Chan, M. K. Y. and Sankaranarayanan, S. K. R. S. (2019b) 'Machine Learning Classical Interatomic Potentials for Molecular Dynamics from First-Principles Training Data', *The Journal of Physical Chemistry C*.

Cheng, L., Redfern, P., Lau, K. C., Assary, R. S., Narayanan, B. and Curtiss, L. A. (2017) 'Computational Studies of Solubilities of LiO2and Li2O2in Aprotic Solvents', *Journal of The Electrochemical Society,* 164(11), pp. E3696-E3701.

Chou, C.-Y. and Hwang, G. S. (2013) 'Lithiation Behavior of Silicon-Rich Oxide (SiO1/3): A First-Principles Study', *Chemistry of Materials,* 25(17), pp. 3435-3440.

Dandu, N., Ward, L., Assary, R. S., Redfern, P. C., Narayanan, B., Foster, I. T. and Curtiss, L. A. (2020) 'Quantum-Chemically Informed Machine Learning: Prediction of Energies of Organic Molecules with 10 to 14 Non-hydrogen Atoms', *The Journal of Physical Chemistry A,* 124(28), pp. 5804-5811.

Dave, A., Mitchell, J., Kandasamy, K., Wang, H., Burke, S., Paria, B., Póczos, B., Whitacre, J. and Viswanathan, V. (2020) 'Autonomous Discovery of Battery Electrolytes with Robotic Experimentation and Machine Learning', *Cell Reports Physical Science,* 1(12), pp. 100264.

Druger, S. D., Nitzan, A. and Ratner, M. A. (1983) 'Dynamic bond percolation theory: A microscopic model for diffusion in dynamically disordered systems. I. Definition and one-dimensional case', *The Journal of Chemical Physics,* 79(6), pp. 3133-3142.

Fan, F., Huang, S., Yang, H., Raju, M., Datta, D., Shenoy, V. B., van Duin, A. C. T., Zhang, S. and Zhu, T. (2013) 'Mechanical properties of amorphous LixSi alloys: a reactive force field study', *Modelling and Simulation in Materials Science and Engineering,* 21(7), pp. 074002.

Franco, A. A., Rucci, A., Brandell, D., Frayret, C., Gaberscek, M., Jankowski, P. and Johansson, P. (2019) 'Boosting Rechargeable Batteries R&D by Multiscale Modeling: Myth or Reality?', *Chemical Reviews,* 119(7), pp. 4569-4627.

Galvez-Aranda, D. E. and Seminario, J. M. (2019) 'Ab Initio Study of the Interface of the Solid-State Electrolyte Li9N2Cl3 with a Li-Metal Electrode', *Journal of The Electrochemical Society,* 166(10), pp. A2048-A2057.

Guo, H., Wang, Q., Stuke, A., Urban, A. and Artrith, N. (2021) 'Accelerated Atomistic Modeling of Solid-State Battery Materials With Machine Learning', *Frontiers in Energy Research,* 9(265).
Hall, L. M., Stevens, M. J. and Frischknecht, A. L. (2012) 'Dynamics of Model Ionomer Melts of Various Architectures', *Macromolecules,* 45(19), pp. 8097-8108.
Islam, M. M., Kolesov, G., Verstraelen, T., Kaxiras, E. and van Duin, A. C. T. (2016) 'eReaxFF: A Pseudoclassical Treatment of Explicit Electrons within Reactive Force Field Simulations', *Journal of Chemical Theory and Computation,* 12(8), pp. 3463-3472.
Jain, A., Ong, S. P., Hautier, G., Chen, W., Richards, W. D., Dacek, S., Cholia, S., Gunter, D., Skinner, D., Ceder, G. and Persson, K. A. (2013) 'Commentary: The Materials Project: A materials genome approach to accelerating materials innovation', *APL Materials,* 1(1), pp. 011002.
Kamath, G., Narayanan, B. and Sankaranarayanan, S. K. R. S. (2014) 'Atomistic origin of superior performance of ionic liquid electrolytes for Al-ion batteries', *Physical Chemistry Chemical Physics,* 16(38), pp. 20387-20391.
Kempaiah, R., Chan, H., Srinivasan, S., Sankaranarayanan, S. K. R. S., Narayanan, B. and Subramanian, A. (2021) 'Impact of Stabilizing Cations on Lithium Intercalation in Tunneled Manganese Oxide Cathodes', *ACS Applied Energy Materials*.
Kim, S.-P., Duin, A. C. T. v. and Shenoy, V. B. (2011) 'Effect of electrolytes on the structure and evolution of the solid electrolyte interphase (SEI) in Li-ion batteries: A molecular dynamics study', *Journal of Power Sources,* 196(20), pp. 8590-8597.
Leung, K. (2012) 'First-Principles Modeling of the Initial Stages of Organic Solvent Decomposition on LixMn2O4(100) Surfaces', *The Journal of Physical Chemistry C,* 116(18), pp. 9852-9861.
Leung, K. and Budzien, J. L. (2010) 'Ab initio molecular dynamics simulations of the initial stages of solid–electrolyte interphase formation on lithium ion battery graphitic anodes', *Physical Chemistry Chemical Physics,* 12(25), pp. 6583-6586.
Leung, K., Qi, Y., Zavadil, K. R., Jung, Y. S., Dillon, A. C., Cavanagh, A. S., Lee, S.-H. and George, S. M. (2011) 'Using Atomic Layer Deposition to Hinder Solvent Decomposition in Lithium Ion Batteries: First-Principles Modeling and Experimental Studies', *Journal of the American Chemical Society,* 133(37), pp. 14741-14754.
Ma, Y. (2018) 'Computer Simulation of Cathode Materials for Lithium Ion and Lithium Batteries: A Review', *ENERGY & ENVIRONMENTAL MATERIALS,* 1(3), pp. 148-173.
Merinov, B. V., Zybin, S. V., Naserifar, S., Morozov, S., Oppenheim, J., Goddard, W. A., Lee, J., Lee, J. H., Han, H. E., Choi, Y. C. and Kim, S. H. (2019) 'Interface Structure in Li-Metal/[Pyr14][TFSI]-Ionic Liquid System from ab Initio Molecular Dynamics Simulations', *The Journal of Physical Chemistry Letters,* 10(16), pp. 4577-4586.
Narayanan, B., Chan, H., Kinaci, A., Sen, F., Gray, S., Chan, M. and Sankaranarayanan, S. (2017) 'Machine learnt bond order potential to model metal-organic (Co-C) heterostructures', *Nanoscale,* 9(46), pp. 18229-18239.
Narayanan, B., Redfern, P. C., Assary, R. S. and Curtiss, L. A. (2019) 'Accurate quantum chemical energies for 133 000 organic molecules', *Chemical Science,* 10(31), pp. 7449-7455.
Nolan, A. M., Zhu, Y., He, X., Bai, Q. and Mo, Y. (2018) 'Computation-Accelerated Design of Materials and Interfaces for All-Solid-State Lithium-Ion Batteries', *Joule,* 2(10), pp. 2016-2046.
Ohwaki, T., Ozaki, T., Okuno, Y., Ikeshoji, T., Imai, H. and Otani, M. (2018) 'Li deposition and desolvation with electron transfer at a silicon/propylene-carbonate interface: transition-state and free-energy profiles by large-scale first-principles molecular dynamics', *Physical Chemistry Chemical Physics,* 20(17), pp. 11586-11591.
Pang, Q., Shyamsunder, A., Narayanan, B., Kwok, C. Y., Curtiss, L. A. and Nazar, L. F. (2018) 'Tuning the electrolyte network structure to invoke quasi-solid state sulfur conversion and suppress lithium dendrite formation in Li–S batteries', *Nature Energy,* 3(9), pp. 783-791.
Patra, T. K., Loeffler, T. D., Chan, H., Cherukara, M. J., Narayanan, B. and Sankaranarayanan, S. K. R. S. (2019) 'A coarse-grained deep neural network model for liquid water', *Applied Physics Letters,* 115(19), pp. 193101.

Persson, K., Sethuraman, V. A., Hardwick, L. J., Hinuma, Y., Meng, Y. S., van der Ven, A., Srinivasan, V., Kostecki, R. and Ceder, G. (2010) 'Lithium Diffusion in Graphitic Carbon', *The Journal of Physical Chemistry Letters,* 1(8), pp. 1176-1180.
Qin, J. and de Pablo, J. J. (2016) 'Ordering Transition in Salt-Doped Diblock Copolymers', *Macromolecules,* 49(9), pp. 3630-3638.
Qu, X., Jain, A., Rajput, N. N., Cheng, L., Zhang, Y., Ong, S. P., Brafman, M., Maginn, E., Curtiss, L. A. and Persson, K. A. (2015) 'The Electrolyte Genome project: A big data approach in battery materials discovery', *Computational Materials Science,* 103, pp. 56-67.
Raju, M., Ganesh, P., Kent, P. R. C. and van Duin, A. C. T. (2015) 'Reactive Force Field Study of Li/C Systems for Electrical Energy Storage', *Journal of Chemical Theory and Computation,* 11(5), pp. 2156-2166.
Schwietert, T. K., Vasileiadis, A. and Wagemaker, M. (2021) 'First-Principles Prediction of the Electrochemical Stability and Reaction Mechanisms of Solid-State Electrolytes', *JACS Au,* 1(9), pp. 1488-1496.
Shin, M., Wu, H.-L., Narayanan, B., See, K. A., Assary, R. S., Zhu, L., Haasch, R. T., Zhang, S., Zhang, Z., Curtiss, L. A. and Gewirth, A. A. (2017) 'Effect of the Hydrofluoroether Cosolvent Structure in Acetonitrile-Based Solvate Electrolytes on the Li+ Solvation Structure and Li–S Battery Performance', *ACS Applied Materials & Interfaces,* 9(45), pp. 39357-39370.
Srinivasan, V., Higa, K., Barai, P. and Xie, Y. (2018) 'Computational Modeling of Morphology Evolution in Metal-Based Battery Electrodes', in Andreoni, W. and Yip, S. (eds.) *Handbook of Materials Modeling : Methods: Theory and Modeling*. Cham: Springer International Publishing, pp. 1-27.
Sun, Y., Kotiuga, M., Lim, D., Narayanan, B., Cherukara, M., Zhang, Z., Dong, Y., Kou, R., Sun, C.-J., Lu, Q., Waluyo, I., Hunt, A., Tanaka, H., Hattori, A. N., Gamage, S., Abate, Y., Pol, V. G., Zhou, H., Sankaranarayanan, S. K. R. S., Yildiz, B., Rabe, K. M. and Ramanathan, S. (2018) 'Strongly correlated perovskite lithium ion shuttles', *Proceedings of the National Academy of Sciences,* 115(39), pp. 9672.
Swift, M. W., Swift, J. W. and Qi, Y. (2021) 'Modeling the electrical double layer at solid-state electrochemical interfaces', *Nature Computational Science,* 1(3), pp. 212-220.
Tang, Z.-K., Tse, J. S. and Liu, L.-M. (2016) 'Unusual Li-Ion Transfer Mechanism in Liquid Electrolytes: A First-Principles Study', *The Journal of Physical Chemistry Letters,* 7(22), pp. 4795-4801.
Urban, A., Seo, D.-H. and Ceder, G. (2016) 'Computational understanding of Li-ion batteries', *npj Computational Materials,* 2(1), pp. 16002.
Van der Ven, A., Thomas, J. C., Xu, Q., Swoboda, B. and Morgan, D. (2008) 'Nondilute diffusion from first principles: Li diffusion in ${\text{Li}}_{x}{\text{TiS}}_{2}$', *Physical Review B,* 78(10), pp. 104306.
Wang, A., Kadam, S., Li, H., Shi, S. and Qi, Y. (2018) 'Review on modeling of the anode solid electrolyte interphase (SEI) for lithium-ion batteries', *npj Computational Materials,* 4(1), pp. 15.
Wang, Q., Zhang, G., Li, Y., Hong, Z., Wang, D. and Shi, S. (2020) 'Application of phase-field method in rechargeable batteries', *npj Computational Materials,* 6(1), pp. 176.
Ward, L., Blaiszik, B., Foster, I., Assary, R. S., Narayanan, B. and Curtiss, L. (2019) 'Machine learning prediction of accurate atomization energies of organic molecules from low-fidelity quantum chemical calculations', *MRS Communications,* 9(3), pp. 891-899.
Ward, L., Dandu, N., Blaiszik, B., Narayanan, B., Assary, R. S., Redfern, P. C., Foster, I. and Curtiss, L. A. (2021) 'Graph-Based Approaches for Predicting Solvation Energy in Multiple Solvents: Open Datasets and Machine Learning Models', *The Journal of Physical Chemistry A,* 125(27), pp. 5990-5998.
Yu, S. and Siegel, D. J. (2017) 'Grain Boundary Contributions to Li-Ion Transport in the Solid Electrolyte Li7La3Zr2O12 (LLZO)', *Chemistry of Materials,* 29(22), pp. 9639-9647.
Yu, X. and Manthiram, A. (2017) 'Electrode–Electrolyte Interfaces in Lithium–Sulfur Batteries with Liquid or Inorganic Solid Electrolytes', *Accounts of Chemical Research,* 50(11), pp. 2653-2660.